

A deep-UV optical frequency comb at 205 nm

E. Peters¹, S. A. Diddams^{1,2}, P. Fendel¹, S. Reinhardt¹, T. W. Hänsch¹,
Th. Udem¹

¹Max Planck Institute of Quantum Optics,
Hans-Kopfermann-Str. 1, D-85748 Garching, Germany

²On leave from the National Institute of Standards and Technology,
325 Broadway, Boulder, Colorado 80305, USA

elisabeth.peters@mpq.mpg.de

Abstract: By frequency quadrupling a picosecond pulse train from a Ti:sapphire laser at 820 nm we generate a frequency comb at 205 nm with nearly bandwidth-limited pulses. The nonlinear frequency conversion is accomplished by two successive frequency doubling stages that take place in resonant cavities that are matched to the pulse repetition rate of 82 MHz. This allows for an overall efficiency of 4.5 % and produces an output power of up to 70 mW for a few minutes and 25 mW with continuous operation for hours. Such a deep UV frequency comb may be employed for direct frequency comb spectroscopy in cases where it is less efficient to convert to these short wavelengths with continuous wave lasers.

© 2009 Optical Society of America

OCIS codes: (140.3610) Lasers, ultraviolet; (190.2620) Harmonic generation and mixing

References and links

1. A. Dubietis, G. Tamošauskas, A. Varanavičius, G. Valiulis, and R. Danielius, "Highly efficient subpicosecond pulse generation at 211 nm," *J. Opt. Soc. Am. B* **17**, 48-52 (2000).
2. A. Nebel and R. Beigang, "External frequency conversion of cw mode-locked Ti : Al₂O₃ laser radiation," *Opt. Lett.* **16**, 1729-1731 (1991); "Tunable picosecond pulses below 200 nm by external frequency conversion of cw modelocked Ti : Al₂O₃ laser radiation," *Opt. Commun.* **94**, 369-372 (1992).
3. K.F. Wall, J.S. Smucz, B. Pati, Y. Isyanova, P.F. Moulton, and J.G. Manni, "A quasi-continuous-wave deep ultraviolet laser source," *IEEE J. Quantum Electron.* **39**, 1160-1169 (2003).
4. F. Rotermund, and V. Petrov, "Generation of the fourth harmonic of a femtosecond Ti:sapphire laser," *Opt. Lett.* **23** 1040-1042 (1998).
5. J. Ringling, O. Kittelmann, F. Noack, G. Korn and J. Squier, "Tunable femtosecond pulses in the near vacuum ultraviolet generated by frequency conversion of amplified Ti:sapphire laser pulses," *Opt. Lett.* **18** 2035-2037 (1993).
6. S. Bourzeix, B. de Beauvoir, F. Nez, F. de Tomasi, L. Julien, and F. Biraben, "Ultra-violet light generation at 205 nm by two frequency doubling steps of a cw titanium-sapphire laser," *Opt. Commun.* **133**, 239-244 (1997).
7. O. Arnoult, F. Nez, C. Schwob, L. Julien, and F. Biraben, "Towards an absolute measurement of the 1S-3S line in atomic hydrogen," *Can. J. Phys.* **83**, 273-281 (2005).
8. B. de Beauvoir, C. Schwob, O. Acef, L. Jozefowski, L. Hilico, F. Nez, L. Julien, A. Clairon, and F. Biraben, "Metrology of the hydrogen and deuterium atoms: Determination of the Rydberg constant and Lamb shifts," *Eur. Phys. J. D* **12**, 61-93 (2000).
9. G. Hagel, F. Nez, and F. Biraben, "Analysis and observation, on an atomic resonance, of the frequency shift due to the length modulation of an optical cavity," *Appl. Opt.* **41**, 7702-7706 (2002).
10. J. Sakuma, Y. Asakawa, T. Sumiyoshi, and H. Sekita, "High-power cw deep-UV coherent light sources around 200 nm based on external resonant sum-frequency mixing," *IEEE J. Sel. Top. Quantum Electron.* **10**, 1244-1251 (2004).
11. Th. Udem, R. Holzwarth, and T.W. Hänsch, "Optical frequency metrology," *Nature* **416**, 233-237 (2002).
12. Ye.V. Baklanov, and V.P. Chebotayev, "Narrow resonances of two-photon absorption of super-narrow pulses in a gas," *Appl. Phys.* **12**, 97-99 (1977).

13. A. Marian, M.C. Stowe, D. Felinto, and J. Ye, "Direct frequency comb measurements of absolute optical frequencies and population transfer dynamics," *Phys. Rev. Lett.* **95**, 023001/1-4 (2005).
14. P. Fendel, S.D. Bergeson, Th. Udem, and T.W. Hänsch, "Two-photon frequency comb spectroscopy of the 6s-8s transition in cesium," *Opt. Lett.* **32**, 701-703 (2007).
15. M.J. Snadden, A.S. Bell, E. Riis, and A.I. Ferguson, "Two-photon spectroscopy of laser-cooled Rb using a mode-locked laser," *Opt. Commun.* **125**, 70-76 (1996).
16. R.W.P. Drever, J.L. Hall, F.V. Kowalski, J. Hough, G.M. Ford, A.J. Munley, and H. Ward, "Laser phase and frequency stabilization using an optical-resonator," *Appl. Phys. B* **31**, 97-105 (1983).
17. H.W. Kogelnik, E.P. Ippen, A. Dienes, and C.V. Shank, "Astigmatically compensated cavities for cw dye lasers," *IEEE J. Quantum Electron.* **8**, 373-379 (1972).
18. G.D. Boyd, and D.A. Kleinman, "Parametric interaction of focused Gaussian light beams," *J. Appl. Phys.* **39**, 3597-3639 (1968).
19. T.W. Hänsch and B. Couillaud "Laser frequency stabilization by polarization spectroscopy of a reflecting reference cavity," *Opt. Commun.* **35**, 441-444 (1980).
20. C. Chen, "Recent advances in deep and vacuum-UV harmonic generation with KBBF crystal," *Opt. Mater.* **26**, 425-429 (2004).
21. C. Chen, Y. Wang, B. Wu, K. Wu, W. Zeng, and L. Yu, "Design and synthesis of an ultraviolet-transparent nonlinear optical crystal $\text{Sr}_2\text{Be}_2\text{B}_2\text{O}_7$," *Nature* **373**, 322-324 (1995).
22. A.V. Smith, "How to select nonlinear crystals and model their performance using SNLO software," *Proc. SPIE* **3928**, 62-69 (2000).
23. Z. Min, R.W. Quandt, R. Bersohn and H.L. Kim "Extended range of second harmonic generation in $\beta - \text{BaB}_2\text{O}_4$," *IEEE J. Quantum Electron.* **34**, 2409 (1998).
24. J.C. Diels and W. Rudolph *Ultrashort Laser Pulse Phenomena*, (Academic, 2006).
25. A.P. Baronavski, H.D. Ladouceur, and J.K. Shaw, "Analysis of cross correlation, phase velocity mismatch, and group velocity mismatches in sum-frequency generation," *IEEE J. Quantum Electron.* **29**, 580-589 (1993).

1. Introduction

Frequency conversion in nonlinear crystals has been used for a long time to convert laser radiation to shorter wavelengths that is difficult, or impossible to generate directly with existing laser systems. In fact the shortest wavelengths of continuous wave (cw) radiation are generated in this way. The limit for this method is set by the phase matching and transparency range of available nonlinear crystals. Among the known crystals β -barium borate BaB_2O_4 (BBO) is transparent down to 185 nm while it can be phase matched for frequency doubling (SHG) to about 205 nm. Other crystals like lithium triborate LiB_3O_5 (LBO) are transparent to even shorter wavelengths (160 nm) but the phase matching cut-off for SHG occurs at a longer wavelength than for BBO. Sum frequency generation can be used for both crystals to reach the transparency cut-off. While previous authors have used this strategy with ps [1, 2, 3] and fs [4, 5] pulses, the required temporal and spatial overlap of two different color pulses adds further complications that may compromise performance, particularly when one desires the enhancement provided by a resonant optical cavity. This seems to be unnecessary if one is interested in wavelengths above the shortest phase matchable for SHG, which is 205 nm in BBO. This is the subject of this work.

A pulsed laser system at this wavelength will be useful for 2-photon excitation of the $1S - 3S$ transition in atomic hydrogen [6, 7]. An improved value of this transition frequency can be used to further test quantum electrodynamics and to reduce the uncertainty of the Rydberg constant [8]. So far the use of cw lasers for spectroscopy of this transition has been plagued by unwanted nonlinearities, such as photo refractivity, that sets in preferably at shorter wavelengths. A cw laser system for 205 nm that has been used by G. Hagel and co-workers [9], developed a strong counter propagating wave at 410 nm within the last doubling cavity in a very short time after locking. Unfortunately this effect has thus far limited the operation to a scanning or pulsed mode of operation. The resulting 4 μs pulses are subject to periodic Doppler shifts arising from the forward and backward motion of the cavity mirror, which yields a double-peaked $1S - 3S$ line shape. Due to nonlinear frequency chirps caused by an intensity dependence of the refractive index of BBO (thermal and Kerr-effect), the average of the two apparent lines does not necessarily agree with the unshifted transition frequency.

While there are other schemes to generate cw 205 nm light that avoid UV enhancement cavities [10], a mode locked pulsed laser might also provide a solution to this problem. Typically nonlinear frequency conversions are very efficient in the ps regime because large peak intensities can be exploited while phase matching bandwidth limitations are not a serious issue. This relaxes the requirements on the enhancement cavity quality. In addition, nonlinear frequency chirps are stationary in a stationary pulse train and should not shift the observed transition frequency in subsequent spectroscopy, although they may reduce the excitation rate. In the frequency domain such a pulse train is described by a frequency comb [11] and a frequency chirp imposed on the pulses is expressed by a phase change of the modes rather than by a frequency change of these modes. Strictly speaking, the non-linear process discussed here is mostly sum frequency generation among the laser modes explaining why the repetition rate is not doubled along with the carrier frequency. Nevertheless we are referring to it as second harmonic generation (SHG).

Using a frequency comb for high resolution 2-photon spectroscopy the modes add pair wise to the energy difference between the ground and excited levels as pointed out by E.V. Baklanov and co-workers a long time ago [12]. Ideally the full set of modes contribute to the excitation rate while the width of an individual mode sets the laser line width. Thus, for 2-photon spectroscopy, a frequency comb can therefore be entirely equivalent to cw excitation [13, 14, 15].

2. Experimental set up

Our frequency quadrupling system starts with 1.6 W of 820 nm from a mode-locked Ti:sapphire laser (Spectra Physics, Tsunami) with a repetition rate of 82 MHz that is pumped by a frequency doubled Nd:vanadate laser (Coherent, Verdi V10). Its pulse duration was determined with a background-free auto correlation (Femtoscope, MC2) to $\tau_\omega = 1.3$ ps. Using an optical spectrum analyzer (Ando, AQ-6315A) we find that the spectrum is best described by a sech^2 function with a bandwidth of $\Delta\nu_\omega = 0.24$ THz indicating a time bandwidth product at the Fourier limited of 0.315.

As shown in Fig. 1 we stabilize this laser to an external reference cavity that is well isolated from acoustics and temperature variations. The required error signal is generated with the Pound-Drever-Hall method [16] while feeding back on a piezo driven folding mirror of the laser. The spectral width of the laser is sufficiently narrow to operate this servo system exactly as in the cw case when the free spectral range of the reference cavity and the pulse repetition rate are at a (small) integer ratio (1:10 in our case). An acousto-optic modulator allows for tuning the laser relative to the reference cavity. Its moderate finesse (≈ 300) allows to additionally lock the repetition rate of the laser to a precise radio frequency reference without impairing the first lock. The built in Gires-Tournois interferometer, which is used to adjust the round trip group delay, can be utilized for this purpose. In this way this laser is frequency stabilized for high resolution spectroscopy [14].

For the first frequency doubling stage (820 nm \rightarrow 410 nm), both LBO and BBO are suitable as they have good transparency and resistance to damage at high average power. While BBO has a 2.6-times larger nonlinear coefficient, we instead choose LBO because of its lower dispersion and smaller walk-off angle ($\delta_{\text{LBO}} = 15.6$ mrad versus $\delta_{\text{BBO}} = 66.8$ mrad). This provides a longer interaction length for better spatial mode profile of the second harmonic. The 10 mm long crystal is Brewster cut with $\theta = 90^\circ$ and $\phi = 29.6^\circ$ for type I phase matching. It is placed in an aluminum mount which is attached to a Peltier element to heat the crystal to 45°C. Even though the temperature of the aluminum mount is measured (sensor AD590) and controlled within 0.1°C we don't have access to the temperature profile inside the crystal.

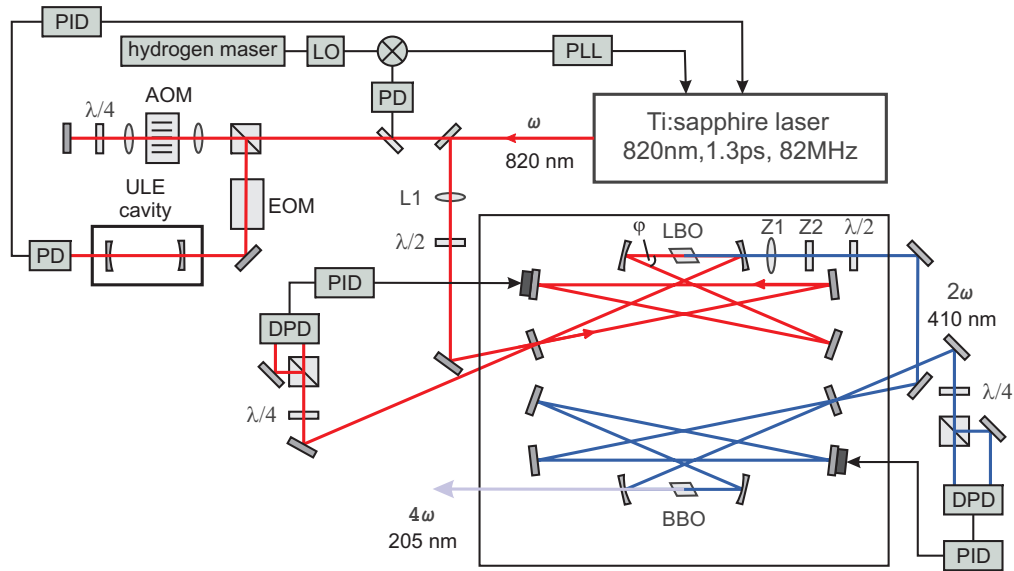


Fig. 1. Experimental setup for deep UV frequency comb generation. A 82 MHz ps mode locked Ti:sapphire laser is stabilized to an external reference cavity and frequency doubled twice with the help of resonant enhancement cavities. The first cavity houses an LBO (820 nm \rightarrow 410 nm) and the second one a BBO crystal (410 nm \rightarrow 205 nm), both of them are Brewster cut. L1: spherical mode matching lens ($f = 2000$ mm); Z1, Z2: cylindrical mode matching lenses ($f_1 = 150$ mm and $f_2 = 230$ mm focusing horizontally and vertically respectively); PD: photo diode; DPD: difference photo diode; EOM: electro-optic modulator; AOM: acousto-optic modulator; ULE: ultra-low-expansion glass; PID: proportional-integral-derivative controller; PLL: phase locked loop, LO: local oscillator.

As shown in Fig. 1 the crystal is placed in a 6 mirror cavity that is arranged to allow full folding angles of $\varphi = 16^\circ$ on the curved mirrors in order to compensate astigmatism [17]. The two focusing mirrors have a radius of curvature of $r=200$ mm, so that an almost spherical beam waist radius of $w_0 = 28 \mu\text{m}$ is obtained. This is somewhat below the optimum focusing condition [18] but helps to limit unwanted nonlinearities. In any case, the single pass conversion efficiency is large enough that the process is conversion loss dominated. In this case, the overall efficiency is independent of the single pass conversion efficiency, provided the proper impedance matching is worked out by picking the correct input coupler transmission. Experimentally we find that a 75 % reflectivity at 820 nm is close to optimum at the given power level of the driving laser, which means that the single pass conversion is around 25%. The remaining mirrors are high reflective at 820 nm ($R > 99.9$ %). The cavity is locked to resonate with the modes of the laser by using the polarization method [19] and feeding back on a piezo-mounted plane folding mirror. Despite Fresnel losses of 20 % for the s-polarized 2nd harmonic at the crystals end facet we obtain 600 mW average power (38 % conversion efficiency) at 410 nm through one of the curved mirrors ($T > 90$ %) uninterrupted for hours.

We are aware of three nonlinear crystals that can be used for the second doubling stage: BBO, $\text{KBe}_2\text{BO}_3\text{F}_2$ (KBBF) [20] and $\text{Sr}_2\text{Be}_2\text{B}_2\text{O}_7$ (SBBO) [21]. The nonlinear coefficient for KBBF is $d_{\text{eff}}(\text{KBBF}) = 0.36$ pm/V [22] and is comparable to the coefficient of BBO $d_{\text{eff}}(\text{BBO}) = 0.35$ pm/V. SBBO should have a comparable or even larger nonlinear coefficient than KBBF [21]. However both KBBF and SBBO are not commercially available, which leaves BBO (Type I: 410 nm (o) \rightarrow 205 nm (e)) as the only present option for us. The phase matching

angle for SHG at 205 nm in BBO of $\theta_{\text{BBO}} = 86.4^\circ$ is unfavorably close to the cut off. We cool the crystal down to -10°C which shifts the phase matching angle by about 1° and increases the effective nonlinearity to $d_{\text{eff}}(\text{BBO}) = 0.35 \text{ pm/V}$ as compared to $d_{\text{eff}}(\text{BBO}) = 0.31 \text{ pm/V}$ at room temperature. Even lower temperatures have been used to further enhance the efficiency [23].

In our set up the BBO crystal is held in a copper mount which is attached to a thermoelectric cooler to servo control its temperature in the same way as the LBO crystal. To prevent condensation and convection we use 32 mm tubes oriented along the laser that are purged with a steady flow of dry oxygen away from the crystal housing.

The 410 nm enhancement cavity is very similar to the first doubling cavity except that the curved mirrors have a radius of curvature of $r = 175 \text{ mm}$ arranged such that they give a $17 \mu\text{m}$ beam waist in the crystal. We find the optimum configuration for the 205 nm light employs an input coupler with 93 % reflectivity, all the other mirrors highly reflective at 410 nm ($R > 99 \%$) and a 5 mm long Brewster-cut BBO crystal. Fresnel losses at the crystals end face amount to 23 %. Nevertheless we extract up to 70 mW of average power at 205 nm through one of the focusing mirrors ($T > 95\%$) albeit for a short period of time only (see below).

3. Results and discussions

There are several effects that can change the pulse duration upon second harmonic generation. For perfect phase matching of all wavelength components and a small input signal, the temporal pulse envelope is simply squared which gives rise to a temporal pulse narrowing by $\sqrt{2}$ for Gaussian pulses and by a factor of 1.45 for sech^2 pulses, without introducing a frequency chirp. However in a real crystal, phase matching can not be achieved for all wavelengths simultaneously so that the second harmonic spectrum $I_2(\Omega)$ is modified. In the plane wave limit we have [24]:

$$I_2(\Omega, L) \sim L^2 \text{sinc}^2 \left\{ \left[\left(\frac{1}{v_2} - \frac{1}{v_1} \right) \Omega + \Delta k \right] \frac{L}{2} \right\} \times I_1^2(\Omega). \quad (1)$$

Here the spectrum of the fundamental wave is given by $I_1(\Omega)$ with the detuning from the carrier frequency Ω for which we can always adjust for proper phase matching, i.e. $\Delta k = 0$. The different frequency dependencies of the refractive indices expressed through the group velocities v_1 and v_2 are limiting the phase matching bandwidth by spectral filtering with the sinc^2 -function. In the time domain the fundamental and SHG pulses separate upon propagation causing a pulse broadening of the latter. Interestingly this pulse broadening does not affect the time bandwidth product in the case of Fourier limited fundamental pulses.

Another pulse broadening effect shows up for larger conversion efficiencies that go beyond the quadratic approximation of Eq. (1). In this case the second harmonic saturates during the peak of the incoming pulse[24]. With no intensity dependent phases these effects do not introduce a chirp. Obtaining essentially chirp free pulses is important for the two photon excitation rate as discussed above.

At the first doubling stage the temporal walk-off of the 820 nm and 410 nm pulses in our 10 mm LBO crystal amounts to 1.1 ps corresponding to a phase matching bandwidth of 0.88 THz defined at the points where the argument of the sinc function in Eq. 1 varies between $\pm\pi$. In addition, due to the large single pass conversion efficiency, some saturation broadening is expected. To verify that these effects go along with a corresponding spectral narrowing, the spectrum at 410 nm was measured with an optical spectrum analyzer and found to possess a nearly sech^2 shape with a width of $\Delta\nu_{2\omega} = 0.32 \text{ THz}$. The pulse duration was then measured by cross correlating the 410 nm pulses with the pulses from the laser by difference frequency generation in a 2.5 mm BBO crystal. Within this crystal the temporal walk-off between the 820 nm and the 410 nm pulses amounts to 0.45 ps with the crossing angle limiting the in-

interaction length to slightly shorter distances. This corresponds to a temporal broadening of the observed cross correlation by $0.315 \times 0.45 \text{ ps} = 0.14 \text{ ps}$ assuming the sech^2 pulse shape is maintained. The duration of the cross correlation can then be calculated from the relation $\tau_{\text{DF}} \approx (\tau_{\omega}^p + \tau_{2\omega}^p + (0.14 \text{ ps})^p)^{(1/p)} = 1.9 \text{ ps}$, with $p = 1.615$ [25] to $\tau_{2\omega} = 1.1 \text{ ps}$. The generated 410 nm pulses are somewhat shorter than the seed pulses albeit not by a factor of 1.45 as expected for a perfect frequency doubler with infinite phase matching bandwidth. The small deviation of the time bandwidth product from the Fourier limit (0.35 rather than 0.315) may be attributed to alignment dependent properties of the laser pulses that causes the initial pulse duration to vary.

In the second doubling cavity the temporal walk-off between the 410 nm and 205 nm pulses is much larger. After the crystal length of $L = 5 \text{ mm}$ they separate by 6.5 ps, so we expect a pulse broadening by approximately $0.315 \times 6.5 \text{ ps} = 2.1 \text{ ps}$ if all pulse shapes are again assumed to maintain their sech^2 envelope. This GVM corresponds to a phase matching bandwidth of 0.15 THz at 410 nm. The resulting spectral bandwidth at 205 nm is determined with a monochromator (Jobin Yvon, HR640) to $\delta\nu_{4\omega} = 0.14 \text{ THz}$ resulting in a Fourier limited pulse duration of 2.2 ps. The actual pulse duration is determined by cross correlating the 205 nm pulses with those at 820 nm. In this case however an even thinner BBO crystal of 0.1 mm thickness was used so that temporal walk-off in the cross correlation can be neglected. Assuming $\tau_{\omega} \ll \tau_{4\omega}$ we determine the pulse duration to be $\tau_{4\omega} = 2.4 \text{ ps}$ giving rise to a time bandwidth product of 0.34. This is close enough to the Fourier limit that it seems safe to assume un-chirped pulses at 205 nm. Figure 2 displays the cross correlations and spectra while Table 1 summarizes the average powers, pulse durations and spectral widths and time bandwidth products (TBP) for all three wavelengths.

Table 1. Overview about the characteristics of the laser system

λ [nm]	$\Delta\nu$ [THz]	NL crystal	output power	acceptance bandwidth	GVM	pulse duration	TBP
820.58	0.24		1.6 W			1.3 ps	0.31
410.29	0.32	LBO	600 mW	0.88 THz	1.1 ps	1.1 ps	0.35
205.15	0.14	BBO	25 mW	0.15 THz	6.5 ps	2.4 ps	0.34

As mentioned above, the maximum power in the deep UV was 70 mW achieved with a 5 mm long BBO crystal. Stability wise we observe several phenomena that prevents the use of the full power for a longer time: Within seconds after locking the second doubling cavity the power drops to about 10 %. Lowering the temperature and/or adjusting the angle of the crystal this output power can be restored. This behavior suggests that heating of the crystal after locking causes a phase mismatch [6]. In addition, after this readjustment a further slower decrease of the power takes place within about 20 minutes settling at around 25 mW. Shifting the crystal transversely regains the power which then drops again within several minutes. The power decrease on the longer time scale might be attributed to the photo chemical reactions at the surface of the crystal that may be reduced under an oxygen atmosphere [6] as described above. Besides we could not observe a counter propagating wave in the cavity, which would indicate photo refractivity. The observed time scales for the power decrease strongly depend on the crystal dimensions. For short crystals of 1 mm and 2 mm length and aperture of $5 \times 5 \text{ mm}^2$ cooling is less efficient resulting in reduced stability.

Our Monte Carlo simulations show that a tightly focused beam at 205 nm of 25 mW should generate a 1S – 3S excitation rate of 10^{-9} per atom in a thermal beam of 6K. However high resolution would require to work with a larger focus in order to reduce time of flight broadening. For this reason we are planning to use a third enhancement cavity at 205 nm which should

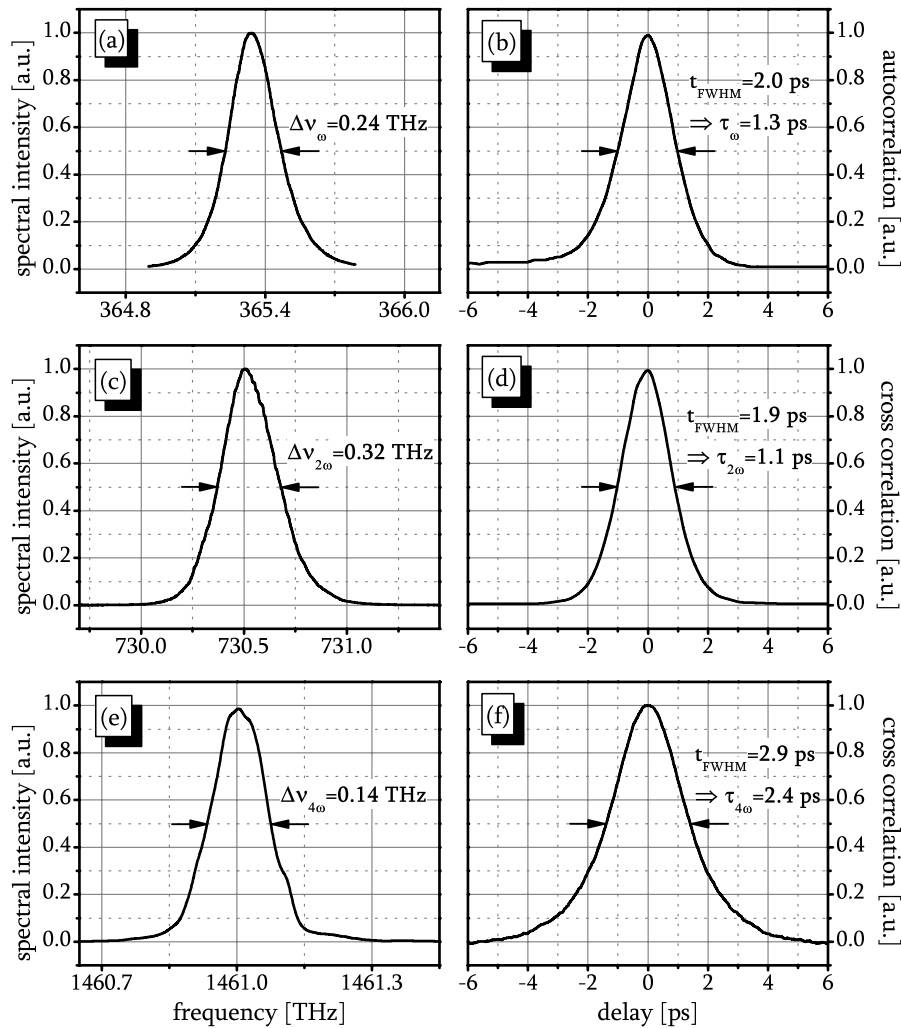


Fig. 2. Power spectra and correlation measurements for the fundamental, second harmonic and fourth harmonic pulses. (a) Power spectrum and (b) auto correlation trace of the fundamental pulses at 820 nm. (c) Power spectrum and (d) cross correlation trace of the second harmonic pulses at 410 nm. (e) Power spectrum and (f) cross correlation trace of the fourth harmonic pulses.

produce a detectable signal. In the future we might optimize the crystal dimensions for lengths and improved thermal contact in order to gain higher UV power with better long term stability. In addition longer pulses might be more efficient for our application, since direct comb spectroscopy is largely independent of pulse duration. Using longer pulses the whole spectrum can be frequency doubled without restrictions due to the phase matching bandwidth, as it is the case for the 1.1 ps pulses at 410 nm.

4. Conclusion

In summary we demonstrated an all solid state deep-UV laser operating at 205 nm suitable for driving the 1S – 3S 2-photon resonance in atomic hydrogen. Starting with an 82 MHz ps laser with 1.6 W at 820 nm a maximum output power of 70 mW at 205 nm is achieved by two resonant second harmonic generation stages with an overall efficiency of 4.5 %. Cross correlation measurements revealed temporal pulse broadening but the corresponding spectral narrowing suggests that essentially un-chirped 2.4 ps pulses at 205 nm are generated.

Acknowledgements

This research was partially supported by the DFG cluster of excellence “Munich Center for Advanced Photonics”.